Many particle simulations of the quantum electron gas using momentum-dependent potentials

W. Ebeling and F. Schautz
Institut für Physik, Humboldt-Universität zu Berlin, Invalidenstraße 110, D-10115 Berlin, Germany
(Received 10 December 1996)

A simple quasiclassical model of the quantum electron gas based on a quasiclassical dynamics with an effective momentum-dependent Hamiltonian is developed. The quantum mechanical effects corresponding to the Pauli and the Heisenberg principles are modeled by constraints in the Hamiltonian. By using the concept of minimum uncertainty wave packets, momentum-dependent effective potentials are derived. Monte Carlo and molecular dynamics calculations are carried out for ensembles of 64–512 electrons and calculations of the internal energy at several temperatures are given. A comparison with quantum Monte Carlo calculations of the mean energy for low temperatures and with Padé approximations for several finite temperatures show that at least in thermodynamic equilibrium our simple model yields reasonable results. [S1063-651X(97)13807-7]

PACS number(s): 52.65.−y, 71.10.Ca, 03.65.Sq, 05.30.Fk

I. INTRODUCTION

The electron gas on a positive background belongs to the most interesting model objects in physics [1–4]. Electrons have strong interactions due to Coulombic forces and strong quantum statistical effects due to the Fermi character. Several limiting cases were treated analytically. Important results on the ground state and the thermodynamical properties at finite temperatures were obtained already in the analytical work of Wigner, Macke, Gell-Mann, and Brueckner (see, e.g., [1–3]). Let us consider now the characteristic length and dimensionless parameters of an electron plasma with density n and temperature T.

Characteristic length parameters: The average distance of the electrons is the Wigner-Seitz radius $d=[3/4\pi n]^{1/3}$; the Bohr radius is defined as $a_B=\hbar/me^2$. Other characteristic lengths are the Landau length $l=e^2/kT$ and the de Broglie wavelength $\Lambda=h/[2\pi mkT]^{1/2}$.

Dimensionless parameters: Furthermore, we define some dimensionless parameters: the Gell-Mann–Brueckner parameter $r_s=d/a_B$, the degeneration parameter Λ/d or $n\Lambda^3$, and the coupling parameter $\Gamma=l/d$.

In the limit when the average distance is large in comparison with the Bohr radius, i.e., if $r_s\geqslant 1$ the electron gas behaves classically. The classical case was treated analytically by Abe and others, Monte Carlo calculations in a wide range of Γ values were carried out e.g., by Brush, Sahlin and Teller, DeWitt, Ichimaru, and other workers (see [1–4]). Quantum corrections to the classical case that are relevant at moderate values of r_s were investigated by De Witt and many others [5–10].

All the analytical calculations mentioned so far cover only limiting cases, such as, e.g., $r_s<1$ or $\Gamma<1$. This is the reason why simulations are of great interest. We mentioned already the extensive Monte Carlo (MC) calculations for the classical region. Classical molecular dynamics (MD) calculations were presented by Hansen *et al.* The particular interest in molecular dynamics calculations is connected with the fact that they also give us access to nonequilibrium properties [11]. For the quantum region the available material is less exhaustive. In particular we mention the Monte Carlo calculations at low temperatures given by Ceperley and Alder [12] and several investigations devoted to the simulation of two-component plasmas [13–16,25,26].

Recently, quasiclassical simulations of many particle systems have received a great deal of interest because of their relative simplicity. As a first example we mention the semiclassical approach to molecular dynamics developed by Hansen *et al.* [11].

In this paper a quasiclassical approach to the quantum electron gas using momentum-dependent potentials is developed. Our approach follows a line of thought developed in the last twenty years by a series of authors, such as, e.g., Heller, Wilets, Kirschbaum, Dorso, and Randrup. In the class of models developed by these authors the quantum effects are approximated by certain constraints in the Hamiltonian [17,18,20].

In an early paper Wilets, Henley, Kraft, and Mackellar [21] proposed a quasiclassical model for nuclear collisions, where the Pauli exclusion principle is simulated by a momentum-dependent two-body interaction. Later Kirschbaum and Wilets incorporated the Heisenberg principle by another momentum-dependent contribution. The hydrogen ground state was reproduced exactly; the ground states of H, He, Li, Ne, and Ar were given better than 15%. Cohen applied this model to atoms with higher Z values and derived reasonable results for the ground states of all atoms up to $Z=38$. In general, the quasiclassical approach based on momentum-dependent potentials gives energies being between Thomas-Fermi and Hartree-Fock calculations. Dorso, Duarte, and Randrup presented quasiclassical simulations for the free Fermi gas by using a Gaussian interaction potential depending on the distance in the phase space [18,19].

The conclusion from the papers cited above is that at least in some approximation quantum mechanical effects and in particular the Heisenberg and the Pauli principles may be incorporated into momentum-dependent potentials.

Such a quasiclassical approach has of course several limits, which are basically connected with the trajectory concept. We mention, for example, the principal difficulty in describing microspic quantum effects such as tunneling, and macroscopic quantum effects such as superfluidity and superconductance. Our aim is only the calculation of standard macroscopic properties, which have a well-defined classical

limit. From this point of view we consider the results obtained so far for momentum-dependent potentials [18–22] as encouraging. The aim of this paper is to transfer this type of model to the macroscopic electron gas.

Let us start our investigation with some general considerations. The main idea of the quasiclassical method is to model the Heisenberg uncertainty and the Pauli exclusion by certain constraints in the phase space. These constraints have to be included in interaction potentials. Potentials are scalar functions depending on particle distances. We consider two electrons with positions r_i, r_j and momenta p_i, p_j. Then we may define scalar distances in different ways, e.g., in coordinate space,

$$r_{ij}=|r_i-r_j|, \tag{1}$$

in momentum space,

$$p_{ij}=|p_i-p_j|, \tag{2}$$

or in phase space,

$$\Delta_{ij}=[(r_{ij}/r_0)^2+(p_{ij}/p_0)^2]^{1/2}. \tag{3}$$

These expressions are possible candidates for the variables on which the potentials are depending. Another potential candidate is the product

$$\kappa_{ij}=|r_i-r_j|*|p_i-p_j|. \tag{4}$$

Indeed these combinations have already been used to incorporate quantum-mechanical effects. In particular the theory of Dorso *et al.* [18] is based on the distance in the phase space Δ_{ij} and Wilets *et al.* [21] use the expression κ_{ij}. In these papers the Pauli exclusion is modeled by the constraint

$$\Delta_{ij}\geqslant 1 \tag{5}$$

with the additional condition that

$$p_0 r_0 \simeq \hbar. \tag{6}$$

Further, the Heisenberg uncertainty is modeled by the constraint

$$\kappa_{ij}\geqslant \hbar. \tag{7}$$

Since both these constraints are formulated in phase space, it seems to be natural to use interaction potentials that depend on phase space distances, contrary to the classical case where in general only distances in space appear.

Since our approach is based on a dynamics in phase space, we will study in the next section the relation between quantum mechanics and phase space representations from a more general point of view.

II. WIGNER REPRESENTATIONS AND DYNAMICS IN PHASE SPACE

Wigner showed that quantum mechanical averages of an observable $\hat{A}$ may be formulated as phase space averages [27,28]:

$$\langle \hat{A} \rangle = \int A(q,p)\rho(q,p,t), \tag{8}$$

where

$$A(q,p)=\exp\left[-\frac{i}{\hbar}\, p\ q\right]\hat{A}\exp\left[+\frac{i}{\hbar}\, p\ q\right]. \tag{9}$$

Here q and p are a set of coordinates and momenta, $A(q,p)$ is the Wigner representation of the observable $\hat{A}$, and $\rho(q,p)$ is the so-called Wigner distribution function. For an N-particle system we have

$$q=r_1,\ldots,r_N, \tag{10}$$

$$p=p_1,\ldots,p_N, \tag{11}$$

where r_i and p_i are the individual coordinates and momenta. The Wigner representation of the Hamilton operator is identical to the classical Hamiltonian (the classical energy) $H(q,p)=T(p)+V(q)$.

If $\hat{\rho}$ is the density operator of the system, then the Wigner distribution function is given by

$$\rho(q,p;t)=\text{const}\times\int \hat{\rho}\left(q+\frac{1}{2}Q,q-\frac{1}{2}Q;t\right)\times\exp\left[-\frac{i}{\hbar}\, Q\ p\right]\ dQ. \tag{12}$$

The Wigner density satisfies an integrodifferential equation, which is equivalent to an infinite order partial differential equation, which reads [28]

$$\partial_t\rho(q,p)=\int K(q,q',p,p')\rho(q',p')dq'dp' \tag{13}$$

with

$$K(q,q',p,p')=\text{const}\times\int \exp[i\tau(p'-p)+i\gamma(q'-q)]\times\hbar^{-1}\left[H\left(q'-\frac{1}{2}\hbar\gamma,\ \ p'+\frac{1}{2}\hbar\tau\right)-H\left(q'+\frac{1}{2}\hbar\gamma,\ \ p'-\frac{1}{2}\hbar\tau\right)\right]\ d\gamma d\tau. \tag{14}$$

A principal problem with the Wigner density is that $\rho(q,p,t)$ is not necessarily positively definite. In other words, $\rho(q,p,t)$ is in general not a probability density. On the other hand, the space distribution as well as the momentum distribution have the character of proper probability densities

$$\rho(q,t)=\int dp\ \ \rho(q,p,t),$$
$$\rho(p,t)=\int dq\ \ \rho(q,p,t). \tag{15}$$

Alternative possibilities to introduce a density in the space of coordinates and momenta were investigated, e.g., by Podlipchuk [29] and Mirbach and Korsch [30]. The Husimi phase space density is defined as the overlap of the wave function with a minimum uncertainty wave packet (also denoted as a coherent state)

$$\psi_0(x) = \text{const} \times \exp\left(-\frac{(x-q)^2}{2r_0^2} + \frac{ipx}{\hbar} \right). \tag{16}$$

Here r_0 is the mean dispersion of the wave function. The Husimi density is non-negative and possesses quite interesting properties with respect to the dynamics [30].

Here we will follow another route: we postulate from the very beginning that—at least in some approximation—a phase space dynamics of Liouville (Hamilton) type can be derived from the exact Wigner equation. A Liouville equation may be obtained by developing the integral kernel K with respect to the variables γ and τ. In the linear approximation the integrodifferential equation for the Wigner function reduces to a first order partial differential equation. This effective Liouville equation generates a non-negative phase space density by the dynamics

$$\partial_t \rho(q,p,t) + \{H(q,p;\hbar), \rho(q,p)\} = 0. \tag{17}$$

According to Klimontovich [28] we may incorporate the Pauli principle into the effective Hamiltonian and find for Fermi particles the quasiclassical Hamiltonian

$$H(q,p;\hbar) = \sum_{k=1}^{N} \frac{p_i^2}{2m_i} + \sum_{k,l=1}^{N} \Phi(r_{kl}) - \frac{1}{(2\pi)^3} \sum_{k,l=1}^{N} \tilde{\Phi}\left(\frac{p_{kl}}{\hbar} \right) \delta(r_{kl}), \tag{18}$$

where $\tilde{\Phi}$ is the Fourier transform of the potential Φ. The effective Hamiltonian $H(q,p;\hbar)$ is the generator of a Hamilton type phase space dynamics. The main problem with simulations on the basis of this Hamilton type dynamics is that, in spite of the fact that the Fermi distribution is a solution of Eq. (17), a simulation will not necessarily converge to it. We just have to remember that any function of H yields a stationary solution of the Liouville equation. Nevertheless we may use the effective Hamiltonian for MC simulations if we introduce the Pauli principle by constraints. For example, we may introduce into discrete step MC simulations the constraint that any step that brings a one-particle state into a Δ ellipse around one other particle $\Delta_{ij} \leqslant 1$ is not carried out. By this additional constraint to the simulations the Fermi distribution is obtained in an elementary way. In fact this constraint leads to a distribution where on average each fermion occupies not more than a volume h^3 in the phase space, which is excluded for other fermions.

So far our effective Hamiltonian does not include quantum effects of Heisenberg type. In this way the question remains to find the best approximative way to reduce the integral Wigner equation to a first order partial differential equation whose characteristics may be interpreted as trajectories in phase space. This approximation should take into account Pauli as well as Heisenberg quantum effects.

In order to get reasonable approximations we have to include further nonclassical features in the dynamics. One possible way is to blow up the phase space by introducing specific quantum variables. This route is chosen in the so-called wave-packet dynamics, which introduces the size and the speed of the spreading of the wave packet as additional variables [17,23–26]. Since this method leads to several difficulties in formulating a statistical mechanics [25,26,31], we try here the alternative way based on effective potentials also called pseudopotentials. The easiest way to introduce Heisenberg quantum effects is to introduce quantum constraints at small distances by certain modifications of the classical potentials [32–34]. Kelbg derived purely space-dependent pseudopotentials for the electron gas that were exact up to the first order in e^2 [32,35].

Deutsch, Hansen and others used pseudopotentials of similar shape but with a simpler representation [13,33,34]. Recently quantum mechanical effective potentials were incorporated into the formalism of integral equations for the pair distribution function [36]. A principal disadvantage of effective potentials depending only on the space coordinates was so far that a Hamiltonian dynamics without momentum-dependent interactions necessarily leads to classical momentum distributions. Since the momentum distribution of the dense electron gas shows strong quantum effects due to the Fermi character of the electrons, we include here momentum-dependent interaction terms. As mentioned already this approach was proposed by Wilets and others [20,21] and the main physical ideas leading to this approach were explained already in the Introduction. The physics of velocity-dependent interactions is not well understood yet but this line of thought has proved to be very successful in practical applications [18–22].

The question of how to determine the ''effective interaction'' $V(q,p)$ for the electron gas will be considered in detail in the next section.

As the main criterion for the choice of a good effective Hamiltonian we will use the condition that for some reference state the distance of the space and momentum distributions generated by the Hamiltonian are as close as possible to the exact distributions for that state:

$$\left\| \int dp \quad \rho_0(p,q) - \rho_0(q) \right\| = \min, \tag{19}$$

$$\left\| \int dq \quad \rho_0(p,q) - \rho_0(p) \right\| = \min. \tag{20}$$

In general we will choose the equilibrium state as the reference state.

In the next section the procedure described above will be applied to the electron gas, which is a model system of great importance for plasma physics and solid state physics.

III. EFFECTIVE ELECTRON-ELECTRON INTERACTION

A. Momentum and space distributions

As we have pointed out above, it is our aim to reproduce both the momentum and the phase space distribution of our system in a good approximation. As is well known, the ideal electron gas is characterized by a Fermi distribution of the momenta:

$$f(p)=\left[\exp\left(\beta\frac{p^2}{2m}-\beta\mu\right)+1\right]^{-1}. \quad (21)$$

Further, the pair distribution in the coordinate space is known [27]. We have, for example, in the degenerate case for two electrons after averaging with respect to the spins

$$g_2(r)=1-\frac{1}{2}\left[\frac{3}{x^3}(\sin x-x\cos x)\right]^2 \quad \text{if} \quad T\ll T_F. \quad (22)$$

In the opposite case of nondegenerate electron the distribution reads

$$g_2(r)=1-\frac{1}{2}\exp\left[-\frac{r^2}{\lambda^2}\right] \quad \text{if} \quad T\gg T_F, \quad (23)$$

where $x=r/r_W$, the Wigner length is $r_W=\hbar/p_F$, the thermal de Broglie length is $\lambda=\hbar/\sqrt{mkT}$, the Fermi momentum is $p_F=\hbar(9\pi/4)^{1/3}/d$, and the Fermi temperature is $T_F=p_F^2/2mk$.

In the general case, which includes the Coulombic interactions, the space and momentum distributions may be expressed by the wave functions

$$S(r_1,\ldots,r_N)=\text{const}\times\sum\exp(-\beta E_n)\times|\Psi_n(r_1,\ldots,r_N)|^2, \quad (24)$$

$$S(p_1,\ldots,p_N)=\text{const}\times\sum\exp(-\beta E_n)\times|\Psi_n(p_1,\ldots,p_N)|^2. \quad (25)$$

We note that the distributions $S(r_1,\ldots,r_N)$ and $S(p_1,\ldots,p_N)$ are often called Slater sums. The Slater sums for Coulombic systems were studied in detail by several authors [2].

We see that with the knowledge of the Slater sums one of the conditions for the phase space density given above [Eqs. (19) and (20)] can be fulfilled in an exact way. For example, we will get exact space distributions in equilibrium by the choice

$$V(r_1,\ldots,r_N)=-kT\ln S(r_1,\ldots,r_N). \quad (26)$$

These potentials were often called quantum statistical effective potentials and were used in calculations of the partition function [2,7,13]. A severe disadvantage of this simplest choice of the effective potentials (26) is, however, that—in spite of the correctness of thermodynamic functions—the momentum distributions are correct only in the Boltzmann limit. Therefore, we have to search for better choices and, in particular, for a correct representation of the Fermi distribution (21) for the momenta. This is the ultimate reason that we decided to model the quantum electron system by a quasiclassical Hamiltonian with the following structure:

$$H=\sum_{i=1}^{N}\frac{p_i^2}{2m}+\sum_{i<j}V_P\left(\frac{r_{ij}}{r_0},\frac{p_{ij}}{p_0}\right)+\sum_{i<j}e^2F\left(\frac{r_{ij}}{r_0},\frac{p_{ij}}{p_0}\right). \quad (27)$$

We have here two kinds of electron-electron interaction: the so-called Pauli potential V_P and a Coulomb interaction modified by a certain function $F(x,y)$. In order to derive effective expressions of this type we follow the general idea to average the Hamilton operator with respect to test wave functions

$$H(q,p;\hbar)=\int d\mathbf{x}\psi_0^*(x)\hat{H}\psi_0(x). \quad (28)$$

The main candidates for the choice of test wave functions are symmetrized or anti-symmetrized combinations of minimum uncertainty wave packets after Eq. (16). Defining an effective Hamiltonian in this way was suggested by the so-called wave-packet dynamics, which has found recently quite successful applications to plasmas [25,26,31,37]. Since minimum wave packets contain at least one free parameter, this choice still gives us some freedom in the effective Hamiltonian that will be used below.

B. Pauli potential

Restricting the calculation described above to pair effects and averaging over the two spin configurations of electrons we get

$$V_P(p,r)=V_0\exp(-\Delta^2)\frac{\Delta^2}{1-\exp(-\Delta^2)}, \quad (29)$$

with

$$V_0=\frac{\hbar^2}{2m\,r_0^2}. \quad (30)$$

This is a two-body interaction depending on the phase-space distance already introduced in the Introduction:

$$\Delta^2=\frac{p^2}{p_0^2}+\frac{r^2}{r_0^2}. \quad (31)$$

In our simulations we used a simplified Pauli potential, which is purely Gaussian as already suggested by Dorso *et al.* [18].

$$V_P(p,r)=V_0e^{-\Delta^2/2}. \quad (32)$$

Figure 1 shows that the Dorso potential is in very good agreement with the spin-averaged Pauli potential obtained from Eq. (28).

In the Dorso potential r_0 and V_0 are considered free parameters. In Sec. III D we will give an estimate for these free parameters with respect to the free Fermi gas. Considering the two-particle relative motion, three different kinds of behavior are observed (Fig. 2): (1) Free motion if the fermions are far apart, (2) distorted motion (scattering), and (3) the ''Pauli-forbidden'' area. Of course, if the particles are initially put in this forbidden area they will remain there. But there is no way for them to get into this area if they have been outside; i.e., the region in phase space forbidden by the Pauli principle is separated from the ''normal'' region by a separatrix.

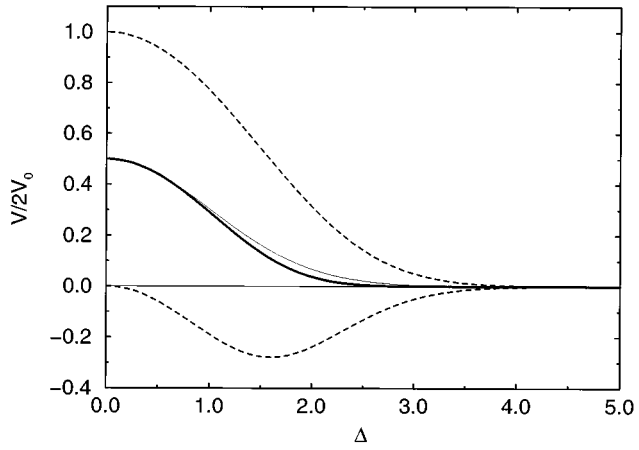

FIG. 1. Comparison of several expressions for the Pauli potential: potential averaged over spins after Eq. (29) (solid line), potential after Eq. (32) (bold line); potential between particles with parallel (upper dashed line) and antiparallel spins (lower dashed line).

C. Coulombic interaction

As already pointed out, we consider here a modified Coulomb interaction rather than the bare Coulomb potential through which purely classical particles would interact. This modification is described by the function F [Eq. (27)]. The procedure of averaging with respect to Gaussian wave functions described above yields

$$F(x,y)=r_0^{-1}\frac{\mathrm{erf}\left(\frac{x}{\sqrt{2}}\right)}{x}-\frac{4\pi}{y^2}\frac{1}{\pi^{3/2}r_0^3}\exp\left\{\frac{-r^2}{r_0^2}\right\}, \quad (33)$$

where $x=r/r_0$ and $y=p/p_0$. In our simulations we used so far only the first momentum-independent contribution, which was obtained already by Klakow *et al.* [25] using Gaussian wave packets [Klakow-Toepffer-Reinhard (KTR) potential]:

$$F(x)=\frac{\mathrm{erf}\left(\frac{x}{\sqrt{2}}\right)}{r_0 x}. \quad (34)$$

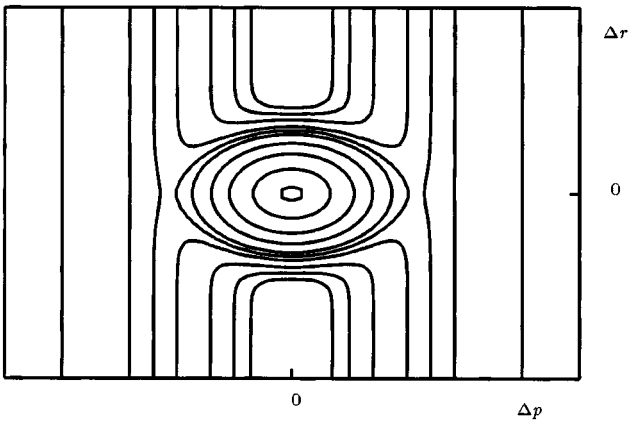

FIG. 2. Lines of constant energy for the two-particle relative motion in the Pauli potential. Depending on the initial phase space distance of the particles three types of motion are observed: free orbits, distorted orbits (scattering), and closed orbits of rather high energy, which therefore contribute little to thermodynamical averages at low temperatures.

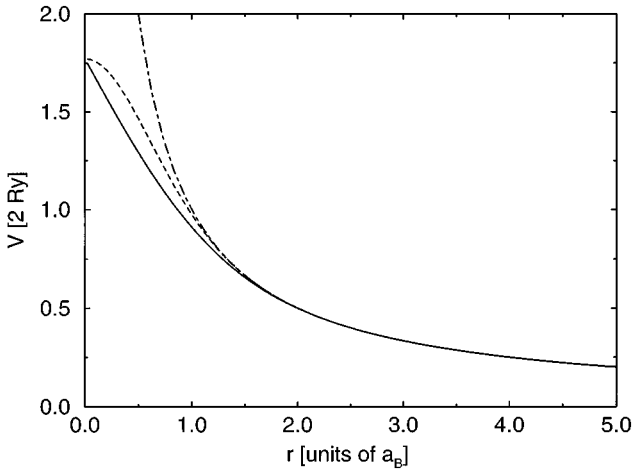

FIG. 3. Different modified Coulomb Interactions: Kelbg potential (solid line) and the wave-packet interaction (dashed line) at short distances. The bare Coulomb potential is also shown (dot-dashed line).

We mention also another expression, which was obtained much earlier by Kelbg [32] using the Slater sum technique

$$F(x)=\{1-\exp(x^2)+\sqrt{\pi}(x)[1-\mathrm{erf}(x)]\}/(r_0 x). \quad (35)$$

In the KTR potential r_0 is connected to the (constant) width of the wave packets and has to be fitted for any particular system. In the Kelbg potential r_0 is equal to the thermal de Broglie wave length $\lambda=\Lambda/\sqrt{2\pi}$. Figure 3 shows the two resulting modified Coulomb potentials. The width of the wave packets was chosen in a way that the two potentials are equal at $r=0$. This leads to the conclusion that at least in the limit of the nondegenerate electron gas, r_0 should be equal to the thermal de Broglie wavelength $r_0=\lambda$.

D. Fitting the free potential parameters

1. The minimal uncertainty condition

Following the approach of minimal uncertainty wave packets we assume that the Heisenberg condition holds as an identity

$$(\delta p_k)(\delta q_k)=\frac{1}{2}\hbar, \quad k=1,2,3. \quad (36)$$

This leads to the relation p_0 by $r_0\ p_0=\hbar$. Further we assume that the momentum uncertainty is given by that of the free Fermi gas

$$(\delta p)^2=2m\epsilon_{\mathrm{kin}}, \quad (37)$$

where ϵ_{kin} is the mean kinetic energy of the free Fermi gas. In this way we get

$$p_0^2=\tfrac{2}{3}\ m\ \epsilon_{\mathrm{kin}}. \quad (38)$$

This condition yields at high temperatures

$$p_0^2=mkT,$$

$$r_0^2=\hbar^2/mkT=\lambda^2, \quad (39)$$

$$V_0 = kT,$$

where λ is the thermal de Broglie wavelength of relative motion. In the limit of low temperatures we get

$$p_0^2 = \tfrac{1}{5}\, p_F^2,$$

$$r_0^2 = \tfrac{5}{2}\left(\frac{4}{9\pi}\right)^{2/3} d^2 \simeq 0.679 d^2, \tag{40}$$

$$V_0 = \tfrac{2}{5}\, \epsilon_F .$$

2. Other estimates for the Pauli potential

At low temperatures Dorso *et al.* gave an estimate for V_0 based on the consideration of $f(p)$ at $T=0$ [18]

$$V_0^{(1)} = \left(\frac{7}{5}\right)^{5/2} \frac{2}{5}\, \epsilon_F \simeq 0.928 \epsilon_F . \tag{41}$$

In the calculation leading to Eq. (41) the Pauli potential V_P is part of the Hamiltonian but is not considered to contribute to the internal energy. Changing this leads to another estimate

$$V_0^{(2)} = \left(\frac{3}{5}\right)^{5/2} \left(\frac{7}{5}\right)^{5/2} \frac{2}{5}\, \epsilon_F \simeq 0.258 \epsilon_F . \tag{42}$$

For r_0 we shall use the value from Eq. (40). In order to improve the expression for V_0 we investigate the pair distribution function $g_2(r)$. In the case of high temperatures we obtain with the Dorso potential

$$g_2^{kl}(r) = \frac{1}{\sqrt{2\pi m k T^3}} \int \int d\vec{p}_1 d\vec{p}_2 \exp[-\beta H_2(\vec{r}_1, \vec{r}_2, \vec{p}_1, \vec{p}_2)] \tag{43}$$

$$g_2^{kl}(r) = 1 - \frac{V_0}{kT} \frac{1}{\sqrt{1 + mkT/2p_0^2}^3} \exp\left(-\frac{r^2}{r_0^2}\right). \tag{44}$$

The comparison with Eq. (23) leads to

$$V_0^{(3)} = \frac{5^{3/2}}{16} kT. \tag{45}$$

This equation may be written as

$$V_0 = \frac{5^{3/2}}{24}\, \epsilon_{\rm kin} . \tag{46}$$

If we extend this relation to low temperatures it yields a third low temperature estimate

$$V_0^{(3)} = \frac{5^{3/2}}{24}\, \epsilon_{\rm kin} \simeq 0.279 \epsilon_F . \tag{47}$$

As we see, this is very similar to the estimate (42). Combining the results given above we see that there exists a temperature T_d at which the high- and low-temperature parameters are continuously connected. An estimate for the transition temperature is $T_d \approx 1.32 \epsilon_F$ and the condition

$$n\lambda^3 = 1 \tag{48}$$

is approximately fulfilled.

In conclusion of this discussion we may state that there is no unique choice for the Pauli potential so far. We need a compromise between the different constraints, which requires density- and temperature-dependent parameters. As far as we can see a good choice is

$$p_0^2 = m\Theta, \quad r_0^2 = \frac{\hbar^2}{4m\Theta}, \quad V_0 = \Theta, \tag{49}$$

where

$$\Theta = \Theta(T,n) = \frac{2}{3}\, \epsilon_{\rm kin}(T,n) \tag{50}$$

is the effective temperature of the free Fermi gas.

IV. MANY PARTICLE SIMULATIONS

A. Monte Carlo and molecular dynamics with MC initial conditions

For equilibrium conditions, Monte Carlo calculations are the easiest way to calculate physical properties, such as, e.g., the average energy. In addition to this method we use here also molecular dynamics, starting with initial conditions obtained from previous Monte Carlo runs.

Usually molecular dynamics simulations addressing equilibrium properties consist of two parts: first the desired temperature is adjusted using some thermostat, while in a second phase the energy is kept constant and measurements are performed.

Since most known thermostats do not work in the case of momentum-dependent interactions, we replaced this first equilibration phase with a MC simulation using the algorithm of Metropolis *et al.* [38]. This algorithm is independent of any particular form of the interaction. To perform the molecular dynamics simulations we used a fourth order Runge-Kutta integrator with step size control. The runs were of length of order 50 times the inverse plasma frequency.

B. Free Fermi gas

As a first step towards the simulation of the electron gas we considered the free Fermi gas. This model consists of classical particles only interacting through the Pauli potential described above. The potential parameters were set according to Sec. III D. Periodic boundary conditions were used. We generated Monte Carlo runs of 2×10^6 configurations using 64 particles. Histograms for the momentum distribution and the radial pair distribution are shown in Figs. 4–7; here Figs. 4 and 5 correspond to the case of a degenerate Fermi gas and Figs. 6 and 7 to a nondegenerate Fermi gas. A comparison with the analytical formulas for the Fermi distribution [Eq. (21)], the Boltzmann distribution, and the radial pair distribution of the degenerate Fermi gas [Eq. (22)], and of the nondegenerate electron gas [Eq. (23)] is made. We mention that the relatively large fluctuations at small distances and/or momenta are due to statistical problems.

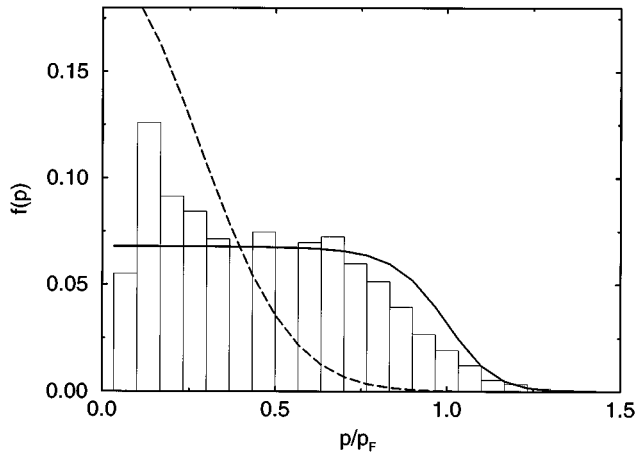

FIG. 4. Momentum distribution function of the free Fermi gas. Results of a simulation with 64 particles, density $n=6.7\times10^{20}$ cm^{-3}, temperature $T=325$ K$=0.1T_F$, potential parameters $V_0=0.26$ eV, $r_0=7.1\times10^{-8}$ cm (histogram), the Fermi-Dirac distribution (solid line) and the Maxwell distribution (dashed line).

C. Electron gas

In order to simulate the ''real'' electron gas the Coulomb interaction is added to the free Fermi gas model. We used the modified Coulomb potential from Eq. (34). The parameter r_0 was set to the value of the parameter r_0 occurring in the Pauli potential. Since our modified Coulomb interaction differs from the bare Coulomb interaction only for short distances the Ewald sum technique for handling the long range part could be used. We carried out several Monte Carlo runs of 2×10^6 for ensembles of 64 electrons embedded in a uniform positive background. The parameters were chosen in such a way that degenerate as well as nondegenerate conditions are covered. For some of the temperature-density pairs used we performed calculations for several numbers of particles up to 512 and extrapolated to infinite particle numbers using a curve of the form $E(N)=a+b/N+c/N^2$, where E is the total energy, N the number of particles, and a,b,c are constants determined by a least-squares fit.

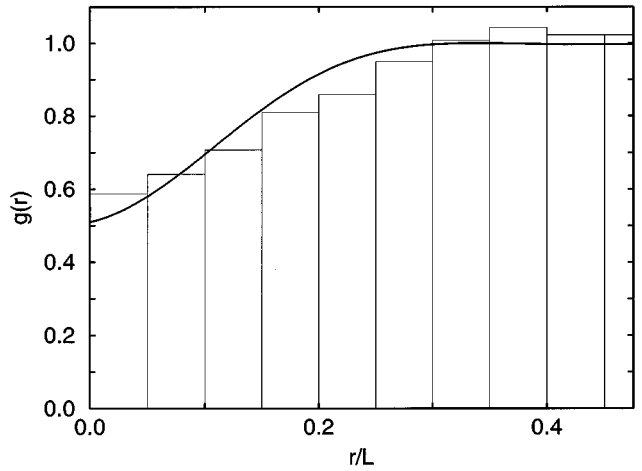

FIG. 5. Radial pair distribution function of the free Fermi gas. Results of a simulation with the same parameters as in Fig. 4 (histogram) and the function $g_2(r)$ from Eq. (22) (solid line). L denotes the size of the basic simulation cell.

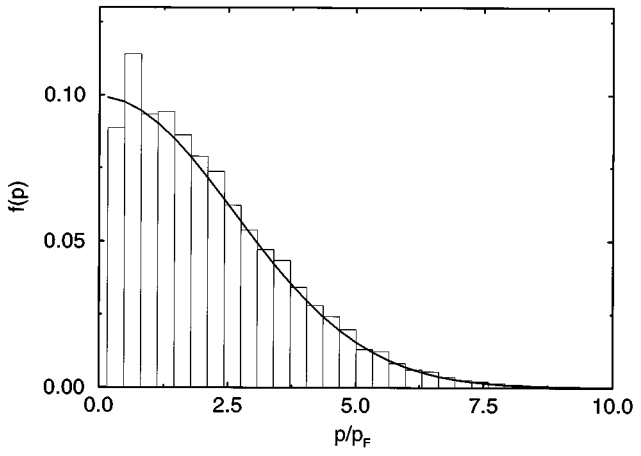

FIG. 6. Momentum distribution function of the free Fermi gas. Results of a simulation with 64 particles, density $n=6.7\times10^{21}$ cm^{-3}, temperature $T=3.5\times10^5$ K$=23T_F$, potential parameters $V_0=21.14$ eV, $r_0=3.5\times10^{-9}$ cm (histogram), and the Fermi-Dirac distribution (solid line).

The results of our simulations are represented in Figs. 8 and 9 and will be compared to the analytical theory in V.

V. COMPARISON WITH THE ANALYTICAL THEORY

A. Analytical formulas for the internal energy

Let us start with the assumption that the energy density of the electron gas can be split into a classical and a quantum mechanical part:

$$u=u_{\mathrm{cl}}+u_{\mathrm{qu}}, \tag{51}$$

where u_{cl} is the energy density of the classical one-component plasma and u_{qu} is by definition the difference between the full and the classical energy density. Explicit calculations for the classical energy of the electron gas were given first by Abe for the low density case. An overview of our analytical and numerical knowledge of the classical energy density as well as a new Padé interpolation formula that connects the low density analytical formulas with the high density MC results was recently given by Kahlbaum [39].

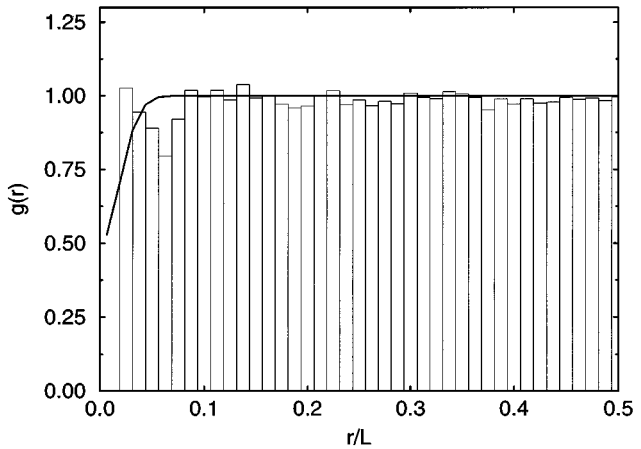

FIG. 7. Radial pair distribution function of the free Fermi gas. Results of a simulation with the same parameters as in Fig. 6 (histogram) and the function $g_2(r)$ from Eq. (23) (solid line).

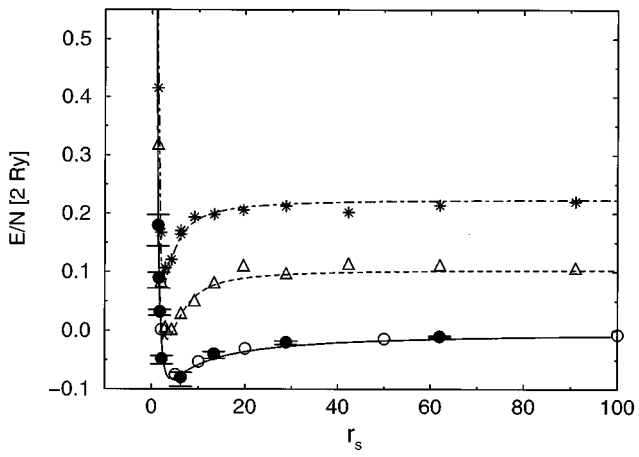

FIG. 8. Electron gas: internal energy per particle as a function of the Gell-Mann–Brueckner parameter r_s: results of our simulations for $T=150$ K (near ground state) (●), $T=22\,000$ K (△), and $T=47\,000$ K (*). The lines show the Padé formula from [44] and the open circles represent results of quantum Monte Carlo simulations [12].

We will consider now the quantum mechanical corrections to the classical energy density and will give a new and very simple derivation of the known result for the quantum effects:

$$u_{\mathrm{qu}}=u-u_{\mathrm{cl}}. \tag{52}$$

According to this splitting we have to consider the difference between the free energy density of a one-component quantum plasma and that of a one-component classical plasma. This expression is convergent and we may, at least in the case of lower density, neglect screening effects. In the low density limit we get

$$u_{qu}=-kTn^2\delta B_2(T). \tag{53}$$

Here $\delta B_2(T)$ is the difference between the quantum and the classical second virial coefficients:

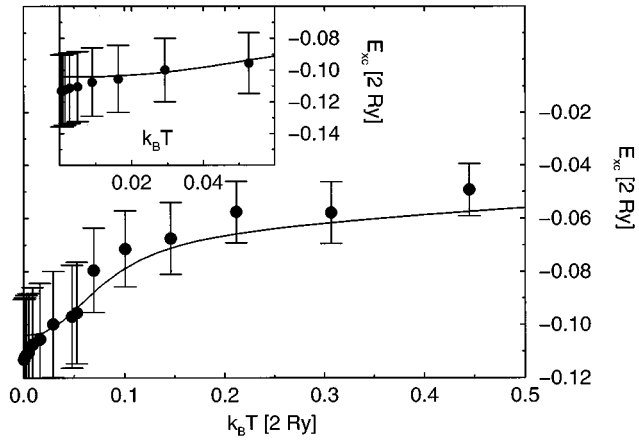

FIG. 9. Electron gas: exchange-correlation energy per particle as a function of the temperature for $r_s=6.2$. Simulations (●) compared to the Padé formula from [44]. The inset shows the low temperature part ($T\leqslant T_d$, $k\ T_d=1.6$ eV, $V_0=1.2$ eV, $r_0=3.3\times10^{-8}$ cm).

$$\delta B_2(T)=[B_2(T)-\lim_{\hbar\to0}B_2(T)]. \tag{54}$$

For this difference function we will find an exact expression by using methods based on the quantum scattering theory [8]. First we transform the two-particle trace to a contour integral over the resolvent. Then the quantum mechanical second virial expression is expressed by

$$B(T)=\frac{\pi^{3/2}\lambda^3}{2i}\int_C\exp(-\beta z)F(z)dz, \tag{55}$$

$$F(z)=\mathrm{Tr}\,\{[\hat{H}-z]-[\hat{H}^0-z]\}. \tag{56}$$

Here $\hat{H}$ is the two-particle Hamiltonian and $\hat{H}^0$ its kinetic part. The full quantum contribution may be found by carrying out the trace using the known Jost functions of the Coulomb scattering problem. We get for the electron gas

$$\delta B_2(T)=2\pi\lambda^3\{Q(-\xi)+DE(-\xi)-(\xi\ 3/6)[\ln(\xi)-D_e]\}. \tag{57}$$

The virial functions Q and E are given by the infinite series that was introduced and discussed first in 1968 [7]. The explicit representations are

$$Q(x)=q_nx^n,\quad E(x)=e_nx^n, \tag{58}$$

$$q_1=-\frac{1}{6},\quad q_2=-\frac{\pi^{1/2}}{8},\quad q_3=\frac{1}{12}-\frac{1}{6}\ln 3-\frac{1}{12}C, \tag{59}$$

$$C=0.577216,\ldots,$$

$$q_n=\frac{\pi^{1/2}\zeta(n-2)}{2^n\Gamma(1+n/2)}\quad\text{if}\quad n\geqslant4. \tag{60}$$

Further

$$e_0=\frac{\pi^{1/2}}{4},\quad e_1=\frac{1}{2},\quad e_2=\frac{\pi^{1/2}}{4}\ln 2,\quad e_3=\frac{\pi^2}{72}, \tag{61}$$

$$e_n=\frac{\pi^{1/2}[1-2^{2-n}\zeta(n-1)]}{2^n\Gamma(1+n/2)}\quad\text{if}\quad n\geqslant4. \tag{62}$$

Similar results as reported here for the electron gas were obtained recently for symmetrical quantum plasmas [40]. The result for the quantum contribution given above is up to the order $O(n^2)$, in full agreement with a result obtained recently by Alastuey and Perez [41]. The next order in the density seems still to be subject to discussions [9,10,42]. Here we shall use only the contribution of the order $O(n^2)$ with which all authors in the field now agree. In the other limit of the strongly degenerated electron gas the known analytical results for the internal energy per electron may be expressed in the form

$$u[ryd]=\frac{2.21}{r_s^2}-\frac{0.916}{r_s}+0.0622\ln r_s-0.096$$
$$+0.018r_s\ln r_s+\cdots. \tag{63}$$

There exist several efforts to connect the known limit cases by Padé approximations. A survey of several Padé approximations was recently given by Stolzmann and Blöcker [43] We shall use here for comparison with the numerical results a formula derived by Ebeling and Lehmann [44].

B. Comparison of analytical and numerical results

In Fig. 8 the internal energy of the electron gas as a function of the Wigner-Seitz radius r_s, i.e., as a function of the density, is shown for several temperatures. The lines represent the values obtained with the Padé formula from [44]. For the density $n=6.7\times10^{21}$ cm^{-3}($r_s=6.2$) Fig. 9 shows the internal energy as a function of the temperature also compared to the Padé formula from [44]. We see that the overall agreement between the analytical formulas and the simulations is rather good. The deviations are all within the error bars of the simulations. Only at the lowest temperatures is a systematic deviation observed (see inset in Fig. 9), which leads to a finite specific heat at $T=0$. We may therefore conclude that at low temperatures and high degeneracy (for $r_s\approx6$ corresponding to $T<10^3$ K) the quasiclassical model developed here breaks down. At conditions of weak or moderate degeneracy, however, our model yields quite reasonable results.

VI. DISCUSSION

We developed in this work a simple quasiclassical model of the quantum electron gas based on a dynamics with an effective momentum-dependent Hamiltonian. The quantum-mechanical effects corresponding to the Pauli and the Heisenberg principles were modeled by constraints in the Hamiltonian. By using the concept of minimum uncertainty wave packets, momentum-dependent effective potentials were derived. The free potential parameters are fitted in such a way that the most important properties of the free electron gas, in particular the momentum-distribution and the pair distribution functions, were described reasonably at least for conditions where the degeneracy is not too strong.

We simulated a many-electron system with periodic boundary conditions by using Monte Carlo and molecular dynamics calculations. Simulations were carried out for ensembles of 64–512 electrons. The mean energy was calculated for several temperatures between 100 and 47 000 K. A comparison with quantum Monte Carlo calculations of the mean energy for low temperatures and with Padé approximations for several finite temperatures shows that at least in thermodynamic equilibrium and moderate degeneracy our simple model yields reasonable results. The main advantage of molecular dynamics simulations in comparison to Monte Carlo methods is that nonequilibrium properties are accessible. As a first example we have given in Fig. 10 the velocity-velocity autocorrelations as a function of the reciprocal plasma frequency. The curves show the typical behavior observed by Hansen, McDonald, and Pollock [11] for the classical electron gas. A more detailed comparison is planned for a forthcoming paper.

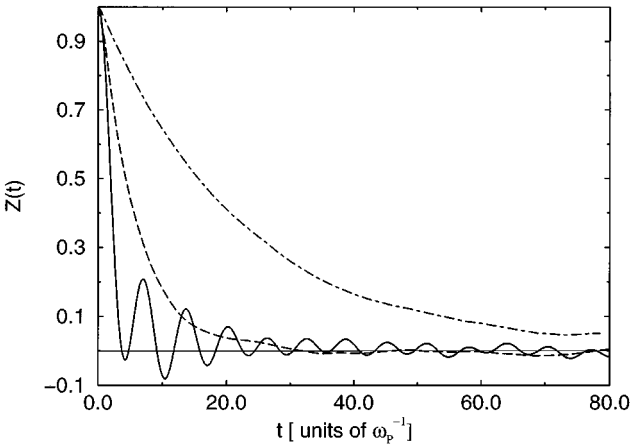

FIG. 10. Velocity autocorrelation functions from MD simulations for $\Gamma=0.15$ (dot-dashed line) and $\Gamma=1.0$ (dashed line), and $\Gamma=60.0$ (solid line).

We cannot expect, however, that the present model, which was obtained by fitting the potential to equilibrium properties, will describe all nonequilibrium properties in a quantitative way. Further improvements of the model might be unavoidable. We may hope, however, that at least near equilibrium some realistic features are still reflected by the model.

ACKNOWLEDGMENT

The authors thank Yu. M. Klimontovich, B. Militzer, V. Podlipchuk, and J. Schnack for helpful discussions.

[1] N.H. March and M.P. Tosi, *Coulomb Liquids* (Academic Press, London, 1984).
[2] W.D. Kraeft, D. Kremp, W. Ebeling, and R. Röpke, *Quantum Statistics of Charged Particle Systems* (Akademie-Verlag, Berlin, 1986).
[3] S. Ichimaru, *Statistical Plasma Physics: I. Basic Principles* (Addison-Wesley, Reading, 1992); *Statistical Plasma Physics II: Condensed Plasmas* (Addison-Wesley, Reading, 1994).
[4] *Physics of Strongly Coupled Plasmas*, edited by W. D. Kraft and M. Schlanges (World Scientific, Singapore, 1996).
[5] H.E. De Witt, J. Math. Phys. **3**, 1216 (1962).
[6] H.J. Hoffmann and W. Ebeling, Physica A **39**, 593 (1968).
[7] W. Ebeling, Ann. Phys. **19**, 104 (1967); **21**, 315 (1968); **22**, 33 (1969); **22**, 383 (1969); **22**, 392 (1969); Physica A **38**, 378 (1968); **40**, 290 (1968); **43**, 293 (1969); **73**, 573 (1974).
[8] W. Ebeling, W.D. Kraeft, and D. Kremp, Beitr. Plasmaphysik **10**, 237 (1970).
[9] W. Ebeling Contr. Plasma Phys. **30**, 553 (1990); **33**, 492 (1993).
[10] J. Riemann, M. Schlanges, H.E. De Witt, and W.D. Kraeft, Physica A **219**, 423 (1995).
[11] J.-P. Hansen, I.R. McDonald, and E.L. Pollock, Phys. Rev. A **11**, 1025 (1975).
[12] D.M. Ceperley and B.J. Alder, Phys. Rev. Lett. **45**, 566 (1980).

[13] V.M. Zamalin, G.E. Norman, and V.S. Filinov, *The Monte Carlo Method in Statistical Mechanics* (Nauka, Moscow, 1977) (in Russian).
[14] J. Clerouin, E.L. Pollock, and P.G. Zarah, Phys. Rev. A **46**, 5130 (1992).
[15] J.I. Penman, J. Clerouin, and P.G. Zerah, Phys. Rev. E **51**, R5224 (1995).
[16] C. Pierleoni, D.M. Ceperley, B. Bernu, and W.R. Magro, Phys. Rev. Lett. **73**, 2145 (1994).
[17] E.J. Heller, J. Chem. Phys. **62**, 1544 (1975).
[18] C. Dorso, S. Duarte, and J. Randrup, Phys. Lett. B **188**, 287 (1987).
[19] C. Dorso and J. Randrup, Phys. Lett. B **215**, 611 (1988).
[20] C.L. Kirschbaum and L. Wilets, Phys. Rev. A **21**, 834 (1980).
[21] L. Wilets, E.M. Henley, M. Kraft, and A.D. Mackellar, Nucl. Phys. **A282**, 341 (1977).
[22] James S. Cohen, Phys. Rev. A **51**, 266 (1995).
[23] H. Feldmeier, Nucl. Phys. **A515**, 147 (1990).
[24] H. Feldmeier, K. Bieler, and J. Schnack, Nucl. Phys. **A586**, 493 (1995).
[25] D. Klakow, C. Toepffer, and P.-G. Reinhard, Phys. Lett. A **192**, 55 (1994).
[26] D. Klakow, C. Toepffer, and P.-G. Reinhard, J. Chem. Phys. **101**, 10 766 (1994).
[27] R.P. Feynman, *Statistical Mechanics* (Benjamin, Reading, MA, 1972).
[28] Yu.L. Klimontovich, *Kinetic Theory of Electromagnetic Processes* (Springer, Heidelberg, 1982); *Kinetic Theory of Nonideal Gases and Nonideal Plasmas* (Academic Press, New York, 1982).
[29] V. Podlipchuk, Teor. Mat. Fiz. **82**, 208 (1990).
[30] B. Mirbach and H.J. Korsch, Phys. Rev. Lett. **75**, 362 (1995).
[31] W. Ebeling and B. Militzer, Phys. Lett. A **221**, 99 (1996).
[32] G. Kelbg, Ann. Phys. (N.Y.) **12**, 219 (1963).
[33] C. Deutsch and M. Lavaud, Phys. Lett. A **39**, 253 (1972); **43**, 193 (1973); **46**, 349 (1974).
[34] J.-P. Hansen and I.K. McDonald, Phys. Rev. A **23**, 2041 (1981).
[35] G. Kelbg, Ann. Phys. (N.Y.) **13**, 354 (1964); **14**, 394 (1964).
[36] D. Beule, W. Ebeling, A. Förster, and M. Kasch, in *Physics of Strongly Coupled Plasmas* (Ref. [4]).
[37] W. Ebeling, A. Förster, and V. Podlipchuk, Phys. Lett. A **218**, 297 (1996).
[38] M. Metropolis, A.W. Rosenblut, M.N. Teller, and E. Teller, Chem. Phys. **21** (1953).
[39] T. Kahlbaum, in *Physics of Strongly Coupled Plasmas* (Ref. [4]).
[40] H. Lehmann and W. Ebeling, Phys. Rev. E **54**, 2451 (1996).
[41] A. Alastuey and A. Perez, Europhys. Lett. **20**, 19 (1992).
[42] A. Alastuey, F. Cornu, and A. Perez, Phys. Rev. E **49**, 1077 (1994).
[43] W. Stolzmann and T. Blöcker, Astron. Astrophys. **226**, 298 (1997).
[44] W. Ebeling and H. Lehmann, Ann. Phys. (N.Y.) **45**, 8 (1988).